Synthesis and Physicochemical Characteristic of Novel Anthracene-Based Building Blocks for Efficient Optical Materials

Dorota Zając	Jadwiga Sołoducho	Tomasz Jarosz
Wrocław University of Science and Technology, Faculty of Chemistry, Wybrzeże Wyspiańskiego 27, 50-370 Wrocław, Poland	Wrocław University of Science and Technology, Faculty of Chemistry, Wybrzeże Wyspiańskiego 27, 50-370 Wrocław, Poland	Centre of Polymer and Carbon Materials of the Polish Academy of Sciences, M. Curie-Sklodowskiej 34, 41-819 Zabrze, Poland Silesian University of Science and Technology, Faculty of Chemistry, Strzody 9, 44-100 Gliwice, Poland

Szczepan Roszak	Mieczysław Łapkowski
Wrocław University of Science and Technology, Faculty of Chemistry, Wybrzeże Wyspiańskiego 27, 50-370 Wrocław, Poland	Centre of Polymer and Carbon Materials of the Polish Academy of Sciences, M. Curie-Sklodowskiej 34, 41-819 Zabrze, Poland Silesian University of Science and Technology, Faculty of Chemistry, Strzody 9, 44-100 Gliwice, Poland

ABSTRACT *Asymmetric (4a-g) antracene-based conjugated compounds comprising electron rich aromatic building blocks were designed and successfully synthesized by the palladium-catalyzed Suzuki coupling and finally by Knoevenagel method. These compounds have a relatively small band gaps and show strong absorption in the region 350-520 nm. Furthermore anthracene based compounds show the light emission in the region from violet to yellow. The electrochemical behavior of synthesized structures was confirmed by EPR as well as theoretical quantum chemical approaches. The calculations rationalize the difference between electrochemical and optical experimentally measured energy gaps.*

Introduction

The anthracene derivatives are widely used in solar cells [1,2], biofuel cells [3], chemosensors [4-6] and above all in organic light-emitting diodes [7-9] as well as organic thin-film transistors [10-12] because of their outstanding photoluminescence, electroluminescence and transport properties, good thermal stability and electrochemical properties. Due to the unique chemical and electron-rich structure, anthracene can be easy modified based on coordination ability of metal ions. The studies on anthracene crystals in the 1960s led to the discovery of organic electroluminescence and it was ensured that anthracene has become an attractive building block for OLEDs [13]. In the 1971 Williams and Schadt reported a 5% quantum efficiency of emission anthracene single-crystal thin films [14,15]. In 1987 the another key achievement was construction of double-layered OLED with suitable organic hole-transport and electron-transport/emissive materials by Tang and Van Slyke [16]. The full-color displays should have the color purity and efficiency of primary red, green, and blue emitting materials. However, still the performance of blue OLEDs is often inferior to that of their red and green counterparts. Cheng et al. reported efficient deep-blue OLEDs with anthracene derivatives as emitters [17]. Laboratories continue to seek effective blue electrofluorescent materials which are energy-saving solid-state lighting that uses in white OLEDs. The previous reports suggest that the unsymmetrical derivatives of anthracene may be a promising structure for the formation of efficient, stable and amorphous films [18-20].

In present work we have designed and synthesized a series of new asymmetric anthracene derivatives (*4a-g*) with an anthracene core and a cyanoacrylic acid group. Electrochemical and photophysical properties for several compounds were studied in details. Density functional theory (DFT) calculations were carried out for all molecules to enhance their understanding of photo-physical and electrochemical properties.

Results and Discussion
Synthesis

Designed novel asymmetric *4a-g* anthracene derivatives were synthesized in three steps procedure (Scheme 1) by Suzuki coupling reaction and then the Knoevenagel method (with piperidine as catalyst) which was a crucial step for the efficiency of the synthesis.

The Knoevenagel condensation involves the coupling of a carbonyl moiety with compounds containing a methylene group activated by one or two electron-withdrawing substituents (nitrile, acyl, or nitro). The liquid-phase Knoevenagel procedure between the C=O functionality and an activated methylene group constitutes an interesting standard way for C–C coupling.

The designed macrostructures *4a-g* were obtained in reaction of 10-(aryl)anthracene-9-carbaldehyde (*3a-g*) and cyanoacetic acid, Scheme 1. After each synthetic step, obtained products were purified by the silica column chromatography. Their structures were confirmed and characterized by standard spectroscopic methods ^{1}H NMR, ^{13}C NMR, MS.
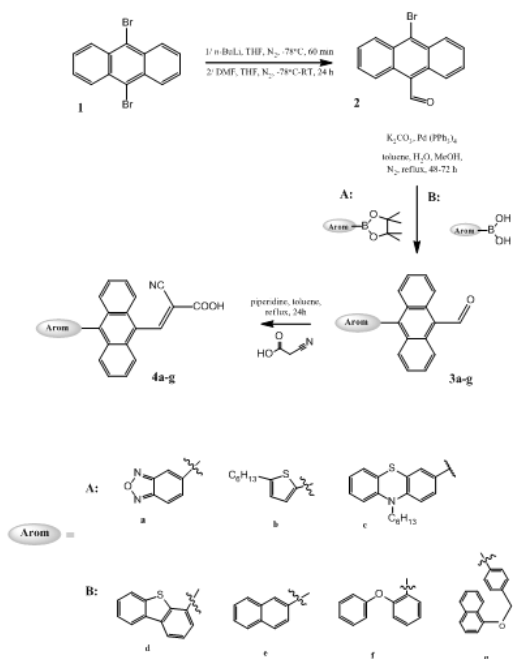
Scheme 1. The synthetic pathway of anthracene-based structures (4a-g).

Electrochemical properties

The electrochemical response of **4a** in dimethyl sulphoxide (Figure 1) consists of a single reversible redox pair centered at -1.68V and an irreversible oxidation signal with an onset at 0.49V. Oxidation to this potential results in the negative potential redox pair not being observed when sweeping towards negative potentials, however, a new irreversible system evolves at -1.04V (Figure 2). This behaviour should result from charge trapping / detrapping, the redox pair at -1.68V would not be affected. Consequently, we have attributed this signal to the reduction of the prod-

ucts of a chemical reaction of the oxidized **4a** molecule, which undergoes specific adsorption on the electrode, affecting the reduction of neutral **4a** on its surface.
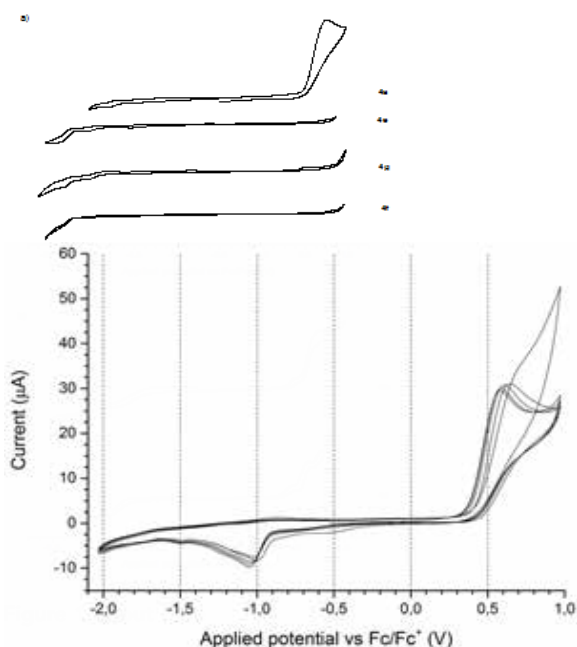

Figure 2. Electrochemical response of 4a with an initial positive potential scan polarity.

The cyclic voltammograms (CV) of **4e**, **4f** and **4g** (Figure 1) all feature redox signals at -1.2÷-1.3V, with **4e** showing partial reversibility and the other two compounds undergoing irreversible reduction. Oxidation of all three compounds proceeds irreversibly, with subsequent scans bringing about a rapid decay of the signal. The energy gaps in all three cases are similar (Table 1), varying from 2.07eV to 2.17eV, which is in line with expectations.

Table 1. Electrochemical and theoretical properties of investigated compounds.

Compound	Reduction potential (V)[a]	Electron affinity (eV)[b]	Oxidation potential (V)[a]	Ionisation energy (eV)[b]	Theor. vertical ionisation energy (eV)	Theor. adiabatic ionisation energy (eV)	Electrochemical frontier orbital energy gap (eV)	Optical frontier orbital energy gap (eV)[c]	HOMO/ LUMO gap (eV)
4a	-1.68	3.42	0.49	5.59	7.29	7.19	2.17	2.76	2.16
4b	-0.56	4.54	1.05	6.15	6.90	6.75	1.61	2.43	2.06
4c	-1.56[d]	3.54	0.22[d]	5.32	6.43	6.32	1.78	2.46	1.06
4d	-0.69	4.41	0.97	6.07	7.49	7.44	1.66	2.63	1.19
4e	-1.33	3.9	0.79	5.89	6.89	6.68	2.12	2.55	1.76
4f	-1.32	3.78	0.85	5.95	7.00	6.83	2.17	2.60	2.97
4g	-1.20	3.9	0.87	5.97	7.01	6.75	2.07	2.61	2.97

The discrepancies in the electrochemical response of the compounds are of low magnitude, as they originate from the exchange of substituents rather than changes to the main conjugated bond system of the molecule. UV-Vis-NIR spectra (Figure 3) supply further evidence to this claim, as the shape of the low energy absorption signal has the same shape for all three compounds, with marginal changes to its maximum absorption wavelength.
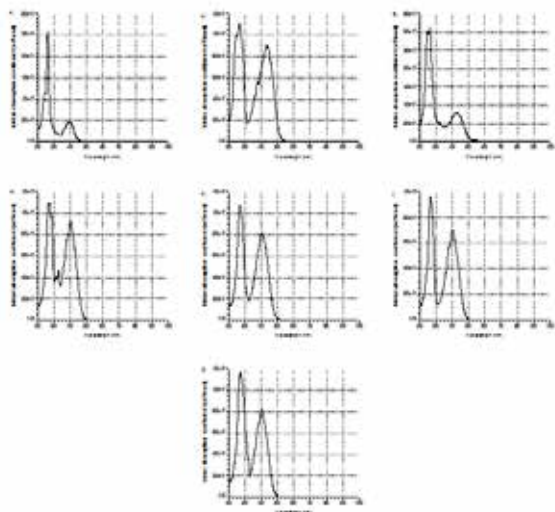

Figure 3. UV-Vis-NIR spectra of investigated compounds a) 4a; b) 4b; c) 4c; d) 4d; e) 4e; f) 4f; g) 4g.

The voltammetric behaviour of *4d* in dichloromethane features a peak at 0.9V and a semi-reversible redox pair centered at 1.08V. Another, irreversible oxidation peak is observed at 1.26V, as is a sharp onset at 1.3V. Upon repeated cycling, the current of the peak at 0.9V increases slightly. Consequently, the signal is attributed to the formation of a product with improved conjugation. Although no electrode deposit is found after the experiment, the formation of a more conjugated product can explain the impaired reversibility of the 1.08V redox pair, which is assumed to arise from the oxidation and reduction of the dibenzothiophene moiety. Upon application of negative potentials, a peak onset at -0.56V is observed, followed by a sequence of three peaks that can be attributed to the reduction of the anthracene moiety. The CV of *4b*, unlike *4d* features irreversible oxidation, which is explained by oxidation of the thiophene moiety and a consecutive chemical reaction. Polymerization and dimerization are excluded, as both α positions of the thiophene ring are blocked. A radical cation localized at one of the β carbons of the thiophene ring, however, it may undergo reaction with the carboxyl group of another *4b* molecule, similar to the mechanism presented in our earlier work for 2-cyano-3-(4-((4-(5-ethylenedioxytiophenyl)phenyl)diphenylsilyl)phenyl)acrylic acid [21]. Reduction occurs much as in the case of *4d*, with a sequence of three reduction peaks being observed for the anthracene moiety. The electrochemical response of *4c* (Figure 4) features both semi-reversible oxidation, with a redox pair, centered at 0.28V and originating from the phenothiazine moiety, and reduction, with a redox pair at -1.65V, arising from the introduction of the first negative charge onto the anthracene moiety.
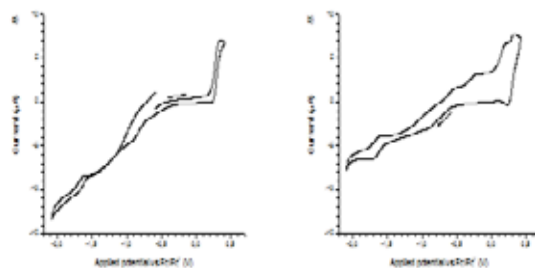

Figure 4. Electrochemical response of 4c dissolved in 0.1M tetrabutylammonium tetrafluoroborate / dichloromethane supporting electrolyte solution: a) initial positive scan polarity; b) initial negative scan polarity. Potential scanning rate r = 0.1 V/s.

Repeated cycling (Figure 4) brings about the evolution of a broad oxidation signal at less positive potentials than those of the phenothiazine redox system, corresponding to the formation of a product featuring extended conjugation length. We have attributed the evolution of this low potential oxidation signal to *4c* dimer, produced by linkage through the phenothiazine moieties. Interestingly, the lack of a reduction signal (accompanying the low potential oxidation peak) indicates that the oxidized dimer is consumed in a consecutive chemical reaction. Due to the presence of both the α-cyanocarboxyllic group in the structure and an electron-rich phenothiazine system to accommodate the intermediate radical cation, we can postulate a coupling mechanism which is similar to the one presented for 2-cyano-3-(4-((4-(5-ethylenedioxytiophenyl)phenyl)diphenylsilyl)phenyl)acrylic acid in our earlier work [21]. Such a mechanism is concurrent with the observed voltammetric curves, since it maintains the conjugation length of the *4c* dimer. Investigation of the radical anions, generated from *4a* (Figure 5a) reveals a rich hyperfine structure. The influence of two nitrogen atoms can be observed, indicating that the radical anion is localized on the benzoxadiazole moiety. Interactions with the neighboring hydrogen atoms of the benzoxadiazole moiety are observed and expected, however, an additional, strong influence of an anthracene hydrogen atom is observed. The theoretically calculated ionization energies (gas phase calculations) reasonably reproduce the measured values. More important the variation of values for different compounds is reproduced confirming the discussion on electrochemical properties.
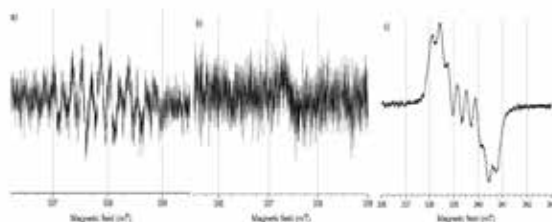

Figure 5. Electron paramagnetic resonance spectra of species electro-generated from the investigated compounds a) 4a radical anion; b) 4f radical anion; c) 4c radical cation.

The EPR spectrum of the *4f* radical anion (Figure 5b) is composed of a single signal, with no developed hyperfine structure. We assume the radical anion is located primarily over the anthracene ring system. Despite several experimental attempts, the EPR signal is weak in intensity,

with a low signal-to-noise ratio. In the case of other investigated compounds, bearing the anthracene moiety, however, only trace signals were found. Seeing that, despite continuing electrolysis only low or trace concentrations of radical anions can be detected, a consecutive chemical reaction is taking place. The reaction in question appears to be hindered through substitution with the phenoxophen-2-yl moiety in *4f*, as we can observe as an EPR signal of the radical anion. Among the substituents to the anthracene moiety present in the investigated compounds, the phenoxophen-2-yl substituent most effectively shields the anthracene moiety sterically, indicating the reaction site. Determining the mechanism of the undergoing reaction, however, requires further investigations, beyond the scope of this work. Similar to the above case, the radical anion of *4c* shows very weak signal intensity and is obscured by the white noise of the apparatus, being observable only through the comparison of integrated spectra. Conversely, the radical cation of *4c* onding to the onset of the *4c* oxidation peak. In this case characteristic line splitting is observed, due to the presence of a nitrogen atom in the system, similar to our earlier work on a phenothiazine derivatives [21, 22].

Optical Spectroscopic Properties

The photophysical properties of the anthracene derivatives were examined in more detail by UV/Vis (Figure 6) and fluorescence (Figure 7) spectroscopy in dichloromethane as solvent at room temperature. The optical properties are summarized in Table 2.
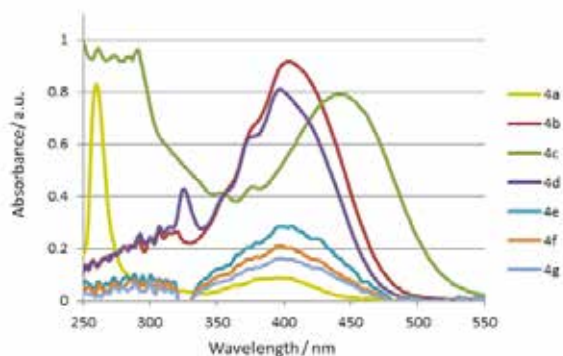

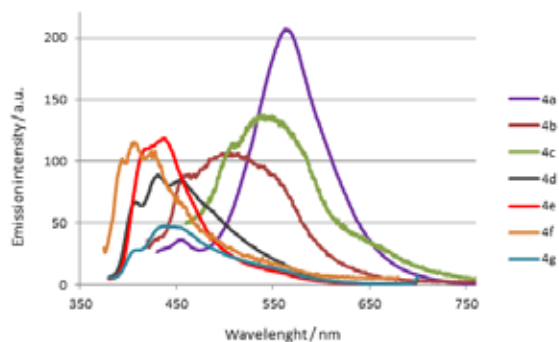**Figure 6. Normalized absorption spectra of the studied compounds in dichloromethane solution (10⁻⁶ mol/dm³).**

Figure 7. Normalized absorption spectra of the studied compounds in dichloromethane solution (10-6 mol/dm3).

The investigated compounds (*4a-g*) show good light absorption covering the region from 350 to 520 nm. For compound *4c*, phenothiazine moiety causes a bathochromic shift of the longest wavelength absorption band to maximum at 444 nm, due to the nitrogen atom, which ex-

erts a strongly electron-withdrawing effect by blue-shifting the high-energy absorption maxima. In solution, the emission maxima λ_{Em} of anthracenes *4d-g* are found in the violet and blue region (380-460 nm), while the compounds *4a-c* are found from blue to yellow region (450-600 nm).
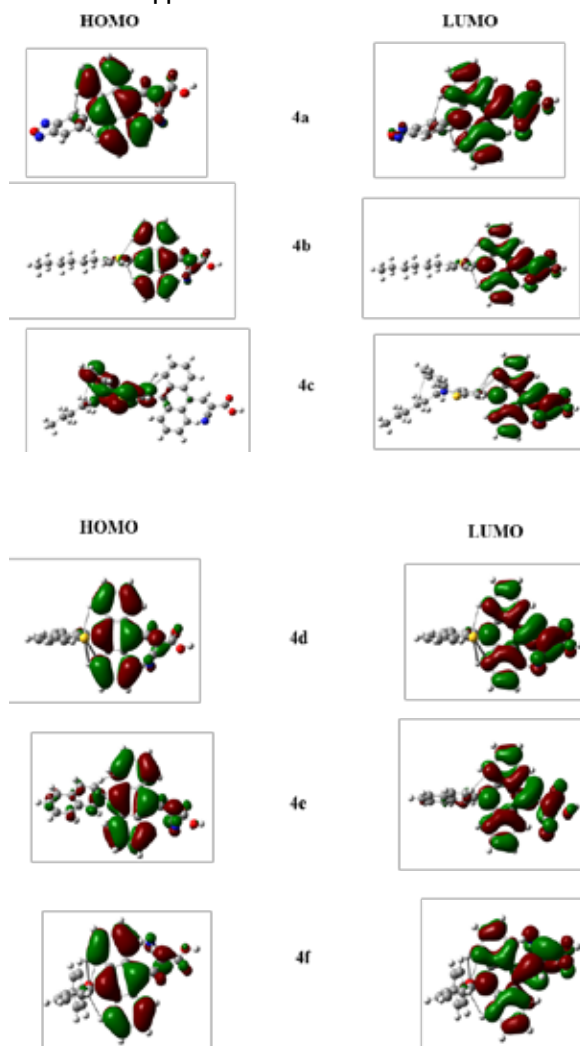
Table 2. Electronic transitions in absorption and emission spectra (nm) and Stokes shift of anthracene derivatives

Macro-structure	λ_{Abs} [nm]	$\lambda_{Abs\ Theoretical}$ [nm]	λ_{Em} [nm]	Stokes shift $\Delta\nu^a$ [cm⁻¹]
4a	397	473 (HOMO→LUMO)	564	74600
4b	404	483 (HOMO→LUMO)	505	4950
4c	444	478 (HOMO→LUMO+1)	540	4004
4d	398	479 (HOMO→LUMO)	431	1920
4e	406	493 (HOMO→LUMO)	438	1800
4f	396	478 (HOMO→LUMO)	406	622
4g	397	477 (HOMO→LUMO+1)	436	2250

a $\Delta\nu = 1/\lambda Abs - 1/\lambda Em$ [cm-1]

Due to the large Stokes shifts [23], there is almost no overlap between absorption and emission bands of the *4a* and *4b* (Table 2), a favorable effect for many applications as blue and green fluorescent dyes.
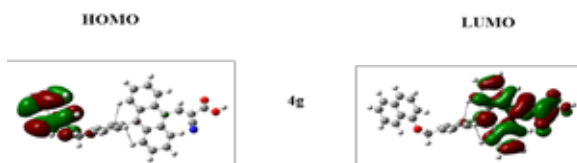
Theoretical Support

Figure 8. HOMOs and LUMOs formation patterns at ground state.

The electronic transitions calculated theoretically overestimate experimental values (Table 2), however, qualitatively confirm the experimental absorption spectra. The orbital picture (Figure 8) indicates the importance of the anthracene ring as a main contributor to the lowest transition of absorption spectra.

Methodological Part
Materials and Instruments
n-Butyllithium (2.5M in hexane), 9,10-dibromoanthracene (98%), tetrakis(triphenylphosphine)-palladium(0) (99%), 3-hexylthiophene-2-boronic acid pinacol ester (95%), phenothiazine (98%), cyanoacetic acid (99%), 2-naphthylboronic acid (95%), 4-[(1-naphthyloxy)methyl]phenylboronic acid (95%), piperidine (99%), anhydrous *N,N*-dimethylformamide (99,8%) were acquired from Sigma-Aldrich. (4,4,5,5-Tetramethyl-1,3,2-dioxaborolan-2-yl)benzofurazan (97%), dibenzothiophene-4-boronic acid (95%), 2-phenoxyphenylboronic acid (95%) were purchased from Acros Organic. Anhydrous potassium carbonate (99%) was received from Chempur. Anhydrous tetrahydrofuran were purchased from POCH. Tetrahydrofuran was dried over Na/benzophenone ketal before used. Dichloromethane (Sigma-Aldrich, CHROMASOLV® 99.9%) was dried and then distilled before the use. Other commercially available chemicals and reagents were used without the prior purification. Preparative column chromatography was performed on the glass column with Fluka silica gel for flash chromatography, 220-440 mesh. 600 MHz ^{1}H NMR and ^{13}C NMR spectra were recorded in deuterated chloroform (CDCl$_3$) and dimethyl sulfoxide (DMSO) on Bruker Avance II 600 Instruments, respectively. Chemical shifts were locked to chloroform δ_H 7.26 (s) and δ_C 77.16 (t) signals and to dimethyl sulfoxide δ_H 2.54 (s) and δ_C 40.00 (m) signals.

The alkyl- and halogen-derivatives (*c*) were obtained by typical protocols [24,25]. Samples for electrochemical and spectroelectrochemical investigation were dissolved in 0.1M tetrabutylammonium tetrafluoroborate (Sigma-Aldrich, >99.0%, electrochemical analysis grade) in dichloromethane (Sigma-Aldrich, CHROMASOLV, >99.9%, HPLC grade) or in dimethyl sulfoxide (Sigma-Aldrich, >99.9%, BioReagent grade), acting as a supporting electrolyte. Each of the compounds was studied individually at a concentration of 1mM.

Electrochemical investigations were performed using a standard three-electrode cell, with a Pt or indium-tin oxide (ITO) working electrode, an Ag pseudo-reference electrode and a Pt coil counter electrode. Measurements were carried out on Metrohm-Autolab PGSTAT100N potentiostat. Prior to measurement, each investigated sample was purged with inert gas, while the same gas was being passed over the experimental solution during the measurement.

UV-Vis-NIR spectroscopic experiments were carried out in a 2mm Hellma QS cuvette. UV-Vis-NIR spectra were reg-istered using an Ocean Optics diode-array spectrometers set (QE65000 and NIRQuest 512). The investigated compounds universally lack absorption signals in the NIR, therefore, the presentation of their spectra is limited to the UV-Vis range for clarity.

Electron Paramagnetic Resonance (EPR) spectra were acquired using a JEOL JES FA-200 X band spectrometer. A capillary spectroelectrochemical cell was used for this purpose, with the same electrode configuration as in the standard electrochemical experiments.

Applied potentials in all of the experiments were calibrated versus the ferrocene/ferrocinium redox couple and, unless stated otherwise, are presented in relation to this reference.

The dilute solutions of derivatives of anthracene in dichloromethane were prepared at a concentration 10^{-6} mol/dm^3. Absorption spectra were gathered with Spectroquant Pharo 300 spectrometer. Fluorescence measurements were performed on the Hitachi F-4500 fluorescence spectrometer.

Synthesis
10-Bromoanthracene-9-carbaldehyde (*2*)
9,10-Dibromoanthracene (*1*) (10.00 g, 29.76 mmol) was dissolved in dry THF and cooled to -78°C. To the solution was dropwise added *n*-BuLi (11.90 ml, 29.76 mmol, 2.5M in hexane). After stirred for 1 h, dimethylformamide (6.91 mL, 89.30 mmol) was added as one portion. Then the reaction mixture was warmed to room temperature and stirred overnight. The reaction was quenched by adding deionized water and the mixture was extracted with diethyl ether. Solvent was evaporated in vacuum and purified with column chromatography using hexane:dichloromethane (7:3) to obtain 5.42 g of an orange solid in 64% yield. Mp: 216-218°C [26].

10-(Benzofurazan-5-yl)anthracene-9-carbaldehyde (*3a*)
To a mixture of *2* (1.00 g, 3.51 mmol), potassium carbonate (1.45 g, 10.50 mmol), and 5-(4,4,5,5-tetramethyl-1,3,2-dioxaborolan-2-yl)benzofurazan (1.04 g, 4.21 mmol) in toluene (50 mL), MeOH (10 mL), and water (10 mL) was added tetrakis(triphenylphosphine)palladium (Pd(PPh$_3$)$_4$) (0.203 g, 0.175 mmol) at room temperature. The resulting mixture was refluxed with stirring 68 h under nitrogen atmosphere. Then the reaction mixture was concentrated under reduced pressure, diluted with water, and extracted with EtOAc. The extract was washed with brine, dried over MgSO$_4$, and concentrated. The residue was purified by silica gel column chromatography using hexane-dichloromethane (7:3) to give *3a* (0.23 g, 20%) as an orange gummy solid.

^{1}H NMR (600 MHz, CDCl$_3$), δ (ppm): δ 11.61 (s, 1H), 9.03 – 9.01 (d, *J* = 12.0 Hz, 2H), 8.11– 8.09 (d, *J* = 12.0 Hz, 1H), 7.97 (s, 1H), 7.74 – 7.72 (t, *J* = 6.0 Hz, 4H), 7.53 – 7.51 (t, *J* = 6.0 Hz, 2H), 7.47 – 7.45 (d, *J* = 12.0 Hz, 1H).

^{13}C NMR (151 MHz, CDCl$_3$) δ 193.45, 149.17, 148.67, 142.07, 141.11, 138.40, 136.80, 136.47, 134.54, 131.77, 131.30, 129.29, 128.83, 127.26, 126.72, 126.58, 124.00, 123.74, 122.01, 118.01, 116.87.

10-(5-Hexylthiophen-2-yl)anthracene-9-carbaldehyde (*3b*)
This compound was prepared by using the same procedure as for bis 10-(benzofurazan-5-yl)anthracene-9-carbaldehyde (*3a*); (1.00 g, 3.51 mmol) of *2*, 3-hexylthiophene-2-boronic acid pinacol ester (*b*) (1.29 g, 4.38 mmol),

potassium carbonate (1.45 g, 10.50 mmol), tetrakis(triphenylphosphine)palladium(0) (0.203 g, 0.175 mmol). The resulting mixture was refluxed with stirring 48 h. The obtained residue was purified by silica gel column chromatography using hexane-dichloromethane (7:3) to give **3b** (1,31 g, 99%) as an yellow gummy solid.

^{1}H NMR (600 MHz, CDCl$_3$), δ (ppm): δ 11.61 (s, 1H), 9.08-9.06 (d, J=12.0 Hz, 2H), 8.01-8.00 (d, J=6.0 Hz, 2H), 7.66-7.64 (t, J=6.0 Hz, 2H), 7.55-7.53 (t, J=6.0 Hz, 2H), 7.03-7.01 (d, J=6.0 Hz, 2H), 2.95-2.93 (t, J=6.0 Hz, 2H), 1.87-1.83 (m, 2H), 1.51-1.47 (m, 2H), 1.41-1.38 (m, 4H), 0.98-0.96 (t, J=6.0 Hz, 3H).

10-(10-Hexyl-10H-phenothiazin-3-yl)anthracene-9-carbaldehyde (3c)

This compound was prepared by using the same procedure as for bis(10-(benzofurazan-5-yl)anthracene-9-carbaldehyde) (**3a**); (1.00 g, 3.51 mmol) of **2**, 3-(4,4,5,5-tetramethyl-1,3,2-dioxaborolan-2-yl)10-hexyl-10H-phenothiazine (**c**) (1.72 g, 4.21 mmol), potassium carbonate (1.45 g, 10.50 mmol), tetrakis(triphenylphosphine)palladium(0) (0.203 g, 0.175 mmol). The resulting mixture was refluxed with stirring 48 h. The obtained residue was purified by silica gel column chromatography using hexane-dichloromethane (7:3) to give **3c** (1,44 g, 84%) as an yellow sticky solid.

^{1}H NMR (600 MHz, CDCl$_3$), δ (ppm): δ 11.60 (s, 1H), 9.03 – 9.02 (d, J = 6.0 Hz, 2H), 7.84 – 7.83 (d, J = 6.0 Hz, 2H), 7.70 – 7.67 (t, J = 9.0 Hz, 2H), 7.47 – 7.44 (t, J = 9.0 Hz, 2H), 7.27 – 7.24 (t, J = 9.0 Hz, 1H), 7.21 – 7.18 (t, J = 9.0 Hz, 3H), 7.10 – 7.08 (d, J = 12.0 Hz, 1H), 7.02 – 6.99 (t, J = 9.0 Hz, 2H), 4.01 – 3.99 (t, J = 6.0 Hz, 2H), 2.00 – 1.95 (m, 2H), 1.58 – 1.55 (t, J = 9.0 Hz, 2H), 1.42 – 1.41 (m, 4H), 0.97 – 0.95 (t, J = 6.0 Hz, 3H).

10-(Dibenzo[b,d]thiophen-4-yl)anthracene-9-carbaldehyde (3d)

This compound was prepared by using the same procedure as for bis(10-(benzofurazan-5-yl)anthracene-9-carbaldehyde) (**3a**); (1.00 g, 3.51 mmol) of **2**, dibenzothiophene-4-boronic acid (**d**) (0.96 g, 4.21 mmol), potassium carbonate (1.45 g, 10.50 mmol), tetrakis(triphenylphosphine)palladium(0) (0.203 g, 0.175 mmol). The resulting mixture was refluxed with stirring 48 h. The residue was purified by silica gel column chromatography using hexane-dichloromethane (7:3) to give **3d** (1,35 g, 99%) as an orange viscous solid.

^{1}H NMR (600 MHz, CDCl$_3$), δ (ppm): δ 11.67 (s, 1H), 9.08 – 9.06 (d, J = 12.0 Hz, 2H), 8.42 – 8.41 (d, J = 6.0 Hz, 1H), 8.33 – 8.32 (d, J = 6.0 Hz, 1H), 7.78 – 7.76 (t, J = 6.0 Hz, 1H), 7.72 – 7.71 (d, J = 6.0 Hz, 1H), 7.70 – 7.69 (d, J = 6.0 Hz, 1H), 7.67 – 7.65 (d, J =12.0 Hz, 2H), 7.55 – 7.53 (m, 2H), 7.50– 7.49 (t, J = 6.0 Hz, 1H), 7.47 – 7.45 (t, J = 6.0 Hz, 1H), 7.42 – 7.39 (t, J = 9.0 Hz, 2H).

10-(Naphthalen-2-yl)anthracene-9-carbaldehyde (3e)

This compound was prepared by using the same procedure as for bis(10-(benzofurazan-5-yl)anthracene-9-carbaldehyde) (**3a**); (1.00 g, 3.51 mmol) of **2**, 2-naphthylboronic acid (**e**) (0.72 g, 4.21 mmol), potassium carbonate (1.45 g, 10.50 mmol), tetrakis(triphenylphosphine)palladium(0) (0.203 g, 0.175 mmol). The resulting mixture was refluxed with stirring 72 h. The residue was purified by silica gel column chromatography using hexane-dichloromethane (7:3) to give **3e** (1,16 g, 99%) as an yellow solid. Mp: 175-176°C.

^{1}H NMR (600 MHz, CDCl$_3$), δ (ppm): δ 11.65 (s, 1H), 9.08 – 9.06 (d, J = 12.0 Hz, 2H), 8.11 – 8.10 (d, J = 6.0 Hz, 1H), 8.07 – 8.05 (d, J = 12.0 Hz, 1H), 7.95 – 7.94 (d, J = 6.0 Hz, 2H), 7.77 – 7.76 (d, J = 6.0 Hz, 2H), 7.72 – 7.69 (t, J = 9.0 Hz, 2H), 7.66 – 7.64 (t, J =6.0 Hz, 2H), 7.55 – 7.54 (d, J =6.0 Hz, 1H), 7.43– 7.41 (t, J = 6.0 Hz, 2H).

10-(2-Phenoxyphenyl)anthracene-9-carbaldehyde (3f)

This compound was prepared by using the same procedure as for bis(10-(benzofurazan-5-yl)anthracene-9-carbaldehyde) (**3a**); (1.00 g, 3.51 mmol) of **2**, 2-phenoxyphenylboronic acid (**f**) (0.98g, 4.56 mmol), potassium carbonate (1.45 g, 10.50 mmol), tetrakis(triphenylphosphine)palladium(0) (0.203 g, 0.175 mmol). The resulting mixture was refluxed with stirring 48 h. The residue was purified by silica gel column chromatography using hexane-dichloromethane (7:3) to give **3f** (1,31 g, 100%) as an yellow viscous solid.

^{1}H NMR (600 MHz, CDCl$_3$), δ (ppm): δ 11.58 (s, 1H), 9.02 – 9.00 (d, J = 12.0 Hz, 2H), 7.86 – 7.84 (d, J = 12.0 Hz, 2H), 7.69 – 7.66 (t, J = 9.0 Hz, 2H), 7.56 – 7.54 (t, J = 6.0 Hz, 1H), 7.50 – 7.47 (t, J = 9.0 Hz, 2H), 7.40 – 7.39 (d, J = 6.0 Hz, 1H), 7.37 – 7.34 (t, J = 9.0 Hz, 1H), 7.15 – 7.11 (m, 3H), 6.95 – 6.92 (t, J = 9.0 Hz, 1H), 6.76 – 6.75 (d, J = 12.0 Hz, 2H).

10-(4-(2-(Naphthalen-1-yloxy)methyl)phenyl)anthracene-9-carbaldehyde (3g)

This compound was prepared by using the same procedure as for bis(10-(benzofurazan-5-yl)anthracene-9-carbaldehyde) (**3a**); (1.00 g, 3.51 mmol) of **2**, 4-[(1-naphthyloxy)methyl]phenylboronic acid (**g**) (1.17 g, 4.21 mmol), potassium carbonate (1.45 g, 10.50 mmol), tetrakis(triphenylphosphine)palladium(0) (0.203 g, 0.175 mmol). The resulting mixture was refluxed with stirring 48 h. The residue was purified by silica gel column chromatography using hexane-dichloromethane (7:3) to give **3g** (1,40 g, 91%) as an yellow viscous solid.

^{1}H NMR (600 MHz, CDCl$_3$), δ (ppm): δ 11.63 (s, 1H), 9.06 – 9.05 (d, J = 6.0 Hz, 2H), 8.50 – 8.48 (t, J = 6.0 Hz, 1H), 7.90 – 7.88 (t, J = 6.0 Hz, 1H), 7.83 – 7.78 (dd, J$_1$ = 12.0 Hz, J$_2$=18.0 Hz, 4H), 7.72 – 7.70 (t, J = 6.0 Hz, 2H), 7.58 – 7.54 (m, 3H), 7.50 – 7.46 (m, 5H), 7.07 – 7.06 (d, J = 6.0 Hz, 1H), 5.47 (s, 2H).

3-(10-(Benzofurazan-5-yl)anthracen-9-yl)-2-cyanoacrylic acid (4a)

In the three necked round bottom flask 10-(benzofurazan-5-yl)anthracene-9-carbaldehyde (**3a**) (0.227 g, 0.700 mmol) was dissolved in toluene (50 ml). Cyanoacetic acid (0.18 g, 2.10 mmol) was added in inert atmosphere of nitrogen. After 15 minutes piperidine (0.070 ml, 0.700 mmol) was added. The resulting mixture was refluxed with stirring overnight. Then the reaction mixture was concentrated under reduced pressure, diluted with water, and extracted with EtOAc. The extract was washed with brine, dried over MgSO$_4$, and concentrated. The residue was purified by silica gel column chromatography using dichloromethane-methanol (95:5) as the eluent to give **4a** (0.072g, 26%) as an yellow solid. Mp: decomposes above 260°C.

^{1}H NMR (600 MHz, DMSO), δ (ppm): δ 8.77 (s, 1H), 8.30 (s, 1H), 8.28-8.27 (d, J=6.0 Hz, 1 H), 8.07-8.05 (d, J=12.0 Hz, 2H), 7.74-7.73 (d, J=6.0 Hz, 2H), 7.68-7.63 (m, 3H), 7.56-7.54 (t, J=6.0 Hz, 2H).

^{13}C NMR (151 MHz, DMSO), δ (ppm): δ 161.92, 149.76, 149.44, 149.10, 148.77, 146.66, 142.75, 141.13, 136.85,

135.41, 130.55, 129.17, 129.08, 128.85, 128.23, 127.91, 127.10, 126.99, 126.85, 126.67, 125.70, 117.07, 116.75, 79.35.

MS (m/z): [M⁺] 390.0885
2-Cyano-3-(10-(5-hexylthiophen-2-yl)anthracen-9-yl)acrylic acid (4b)
This compound was prepared by using the same procedure as for 3-(10-(benzofurazan-5-yl)anthracen-9-yl)-2-cyanoacrylic acid (*4a*); (1.32 g, 3.54 mmol) of 10-(5-hexylthiophen-2-yl)anthracene-9-carbaldehyde (*3b*), cyanoacetic acid (0.904 g, 10.60 mmol), piperidine (0.35ml, 3.54 mmol). The residue was purified by silica gel column chromatography using dichloromethane-methanol (95:5) as the eluent to give *4b* (1.40g, 90%) as a brick red solid, Mp: 174-176°C.

¹H NMR (600 MHz, CDCl₃), δ (ppm): δ 9.49 (s, 1H), 8.08-8.06 (d, J=12.0 Hz, 2H), 8.03-8.02 (d, J=6.0 Hz, 2H), 7.66-7.63 (t, J=9.0 Hz, 2H), 7.54-7.52 (t, J=6.0 Hz, 2H), 7.05 (s, 1H), 7.02 (s, 1H), 3.02-2.99 (t, J=6.0 Hz, 2H), 1.89-1.83 (m, 2H), 1.55-1.51 (m, 2H), 1.44-1.42 (m, 4H), 0.99-0.97 (t, J=6.0 Hz, 3H).

¹³C NMR (151 MHz, CDCl₃), δ (ppm): δ 166.25, 157.67, 148.07, 134.99, 134.75, 131.42, 131.26, 129.65, 128.67, 128.08, 127.83, 127.48, 127.03, 126.13, 125.94, 125.64, 124.45, 124.28, 124.14, 113.72, 112.40, 31.73, 31.69, 31.66, 30.30, 28.99, 22.67, 14.17.

MS (m/z): [M⁺] 440.1673
2-Cyano-3-(10-(10-hexyl-10H-phenothiazin-3-yl)anthracen-9-yl)acrylic acid (4c)
This compound was prepared by using the same procedure as for 3-(10-(benzofurazan-5-yl)anthracen-9-yl)-2-cyanoacrylic acid (*4a*); (1.44 g, 2.95 mmol) of 10-(10-hexyl-10H-phenothiazin-3-yl)anthracene-9-carbaldehyde (*3c*), cyanoacetic acid (0.75 g, 8.84 mmol), piperidine (0.30 ml, 2.95 mmol). The residue was purified by silica gel column chromatography using dichloromethane-methanol (95:5) as the eluent to give *4c* (1.57 g, 96%) as a dark red oil.

¹H NMR (600 MHz, CDCl₃), δ (ppm): δ 9.55 (s, 1H), 8.06 – 8.05 (d, J = 6.0 Hz, 2H), 7.87 – 7.86 (d, J = 6.0 Hz, 2H), 7.66 – 7.64 (t, J = 6.0 Hz, 2H), 7.49 – 7.46 (t, J = 9.0 Hz, 2H), 7.28 – 7.21 (m, 4H), 7.12 – 7.10 (d, J = 12.0 Hz, 1H), 7.02 – 7.00 (t, J = 6.0 Hz, 2H), 4.02 – 4.00 (t, J = 6.0 Hz, 2H), 2.01 – 1.99 (m, 2H), 1.60 – 1.55 (m, 2H), 1.43– 1.40 (m, 4H), 0.97 – 0.95 (t, J = 6.0 Hz, 3H).

¹³C NMR (151 MHz, CDCl₃) δ (ppm): δ 165.53, 157.61, 145.23, 145.05, 141.24, 131.86, 130.00, 129.98, 129.64, 128.87, 128.24, 127.64, 127.46, 127.44, 125.77, 124.99, 124.69, 124.61, 122.66, 115.59, 115.14, 113.89, 112.09, 112.07, 112.03, 111.56, 47.72, 31.57, 27.00, 26.80, 22.68, 14.08.

MS (m/z): [M⁺] 555.2100
2-Cyano-3-(10-(dibenzo[b,d]thiophen-4-yl)anthracen-9-yl)acrylic acid (4d)
This compound was prepared by using the same procedure as for 3-(10-(benzofurazan-5-yl)anthracen-9-yl)-2-cyanoacrylic acid (*4a*); (1.36 g, 3.50 mmol) of 10-(dibenzo[b,d]thiophen-4-yl)anthracene-9-carbaldehyde (*3d*), cyanoacetic acid (0.89 g, 10.50 mmol), piperidine (0.35 ml, 3.50 mmol). The residue was purified by silica gel column chromatography using dichloromethane-methanol (95:5) as the eluent to give *4d* (0.54 g, 34%) as an orange solid, Mp: 294-295°C.

¹H NMR (600 MHz, CDCl₃), δ (ppm): δ 9.40 (s, 1H), 8.65 – 8.64 (d, J = 6.0 Hz, 1H), 8.54 – 8.52 (d, J = 12.0 Hz, 1H), 8.15 – 8.14 (d, J = 6.0 Hz, 2H), 7.85 – 7.83 (t, J = 6.0 Hz, 2H), 7.69 – 7.66 (t, J = 9.0 Hz, 3H), 7.59– 7.56 (t, J = 9.0 Hz, 1H), 7.53 – 7.48 (m, 5H).

¹³C NMR (151 MHz, DMSO) δ (ppm): δ 162.60, 155.34, 140.84, 139.06, 137.18, 136.09, 135.67, 133.00, 132.76, 130.01, 129.72, 129.04, 128.93, 128.47, 128.02, 127.83, 127.65, 127.17, 127.35, 126.82, 126.57, 125.99, 125.47, 123.54, 122.95, 122.49, 122.37, 117.20, 115.84, 115.33.

MS (m/z): [M⁺] 456.1053
2-Cyano-3-(10-(naphthalen-2-yl)anthracen-9-yl)acrylic acid (4e)
This compound was prepared by using the same procedure as for 3-(10-(benzofurazan-5-yl)anthracen-9-yl)-2-cyanoacrylic acid (*4a*); (1.01 g, 3.05 mmol) of 10-(naphthalen-2-yl)anthracene-9-carbaldehyde (*3e*), cyanoacetic acid (0.778 g, 9.15 mmol), piperidine (0.30 ml, 3.05 mmol). The residue was purified by silica gel column chromatography using dichloromethane-methanol (95:5) as the eluent to give *4e* (1.02 g, 84%) as a dark orange solid, Mp: 131−133°C.

¹H NMR (600 MHz, DMSO), δ (ppm): δ 9.36 (s, 1H), 8.18-8.17 (d, J=6.0 Hz, 1H), 8.12-8.10 (t, J=6.0 Hz, 3H), 8.02 (s, 1H), 8.00-7.99 (d, J=6.0 Hz, 1H), 7.65-7.62 (m, 6H), 7.57-7.56 (d, J=6.0 Hz, 1H), 7.48-7.45 (t, J=9.0 Hz, 2H).

¹³C NMR (151 MHz, DMSO), δ (ppm): δ 162.70, 155.39, 139.96, 135.69, 135.59, 133.41, 132.90, 130.17, 129.69, 129.56, 129.20, 128.64, 128.48, 128.34, 128.30, 127.76, 127.57, 127.46, 127.22, 127.09, 126.89, 126.66, 126.39, 125.79, 125.69, 117.25, 115.56, 115.38.

MS (m/z): [M⁺] 400.1346
2-Cyano-3-(10-(2-phenoxyphenyl)anthracen-9-yl)acrylic acid (4f)
This compound was prepared by using the same procedure as for 3-(10-(benzofurazan-5-yl)anthracen-9-yl)-2-cyanoacrylic acid (*4a*); (1.32 g, 3.52 mmol) of 10-(2-phenoxyphenyl)anthracene-9-carbaldehyde (*3f*), cyanoacetic acid (0.90 g, 10.58 mmol), piperidine (0.35 ml, 3.50 mmol). The residue was purified by silica gel column chromatography using dichloromethane-methanol (95:5) as the eluent to give *4f* (0.46 g, 30%) as an orange solid, Mp: 133−135°C.

¹H NMR (600 MHz, DMSO), δ (ppm): δ 9.44 (s, 1H), 8.00-7.99 (d, J=6.0 Hz, 2H), 7.82-7.81 (d, J=6.0 Hz, 2H), 7.56-7.54 (t, J=6.0 Hz, 3H), 7.44-7.41 (m, 3H), 7.37-7.35 (t, J=6.0 Hz, 1H), 7.18-7.17 (d, J=6.0 Hz, 1H), 7.09-7.06 (t, J=9.0 Hz, 2H), 6.89-6.87 (t, J=6.0 Hz, 1H), 6.72-6.71 (d, J=6.0 Hz, 2H).

¹³C NMR (151 MHz, DMSO) δ (ppm): δ 162.66, 162.08, 156.57, 156.53, 156.12, 154.37, 135.98, 133.41, 130.67, 130.53, 130.26, 129.71, 129.62, 128.66, 128.31, 127.74, 127.38, 127.22, 127.13, 126.69, 126.60, 126.31, 125.87, 125.70, 124.07, 119.49, 118.79, 117.46, 115.69, 79.66.

MS (m/z): [M⁺] 442.1427
2-Cyano-3-(10-(4-(2-(naphthalen-1-yloxy)methyl)phenyl)anthracen-9-yl)acrylic acid (4g)
This compound was prepared by using the same procedure as for 3-(10-(benzofurazan-5-yl)anthracen-9-yl)-2-cyanoacrylic acid (*4a*); (1.40 g, 3.19 mmol) of 10-(4-(2-(naphthalen-1-yloxy)methyl)phenyl)anthracene-9-carbaldehyde (*3g*), cyanoacetic acid (0.81 g, 9.57 mmol), piperidine (0.32

ml, 3.20 mmol). The residue was purified by silica gel column chromatography using dichloromethane-methanol (95:5) as the eluent to give **4g** (0.49 g, 31%) as an orange solid, Mp: 288–290°C.

^{1}H NMR (600 MHz, DMSO), δ (ppm): δ 9.30 (s, 1H), 8.36-8.35 (d, J=6.0 Hz, 1H), 8.10-8.09 (d, J=6.0 Hz, 2H), 7.93-7.92 (d, J=6.0 Hz, 1H), 7.87-7.86 (d, J=6.0 Hz, 2H), 7.67-7.66 (d, J=6.0 Hz, 4H), 7.58-7.51(m, 8H), 7.23-7.22 (d, J=6.0 Hz, 1H), 5.52 (s, 2H).

^{13}C NMR (151 MHz, DMSO) δ (ppm): δ 162.66, 154.79, 154.74, 154.71, 154.32, 139.69, 137.67, 137.51, 137.48, 137.37, 134.62, 131.41, 129.50, 129.44, 128.33, 128.13, 128.08, 127.73, 127.46, 127.44, 127.17, 127.03, 126.69, 126.64, 126.37, 125.98, 125.70, 125.64, 125.57, 122.12, 120.80, 177.36, 115.59, 106.35, 69.79.

MS (m/z): [M[+]] 506.1924

Detailes of Theoretical Studies

The presented theoretical studies are based on the density functional theory (DFT) methodology [27]. The DFT approach applied here utilizes the Becke's three-parameter functional [28] with the Vosco et al. local correlation part [29] and the Lee et al. [30] nonlocal part, abbreviated as B3LYP. Calculations were performed using the cc-pVDZ basis set [31]. The energies of excited states were calculated within the time-dependent density functional theory (TDD-FT) [32]. Ten excited stated were included in calculations. The computations were carried out using *Gaussian-09* suite of codes [33]. The molecular graphic was produced applying the *GaussView* software [34].

Conclusions and Remarks

The synthesis and the investigation of macrocyclic structures based on anthracene are reported. These compounds were synthesized by the Knoevenagel procedure with high yield. All compounds are electronically and optically active. Studied compounds, in solution, show good light absorption covering the region up to 520 nm. Furthermore, the asymmetric compounds (*4a-g*) show the light emission in region from violet to yellow. The cyclic voltammetry was employed to characterize the electrochemical behavior. The onset of the oxidation wave was found at rather low potentials. The optical band gap, between 2.43 eV and 2.76 eV, makes the structures potentially useful as an hosting material for emitters and hole/electron blocking layer in the OLEDs displays. The lowest electrochemical and optical band gap characterizes asymmetric structure containing thiophene unit, the largest - structure with benzofurazane moiety. Electrochemical properties of investigated compounds make this material of interest for electrochromic applications.

Although, EPR spectra provide little information about the structure of the electro-generated radical anions, it excludes any significant degree of communication between radical anions present on anthracene fragment of *4f*. It was assumed that the radical anion is located primarily over the anthracene ring system. In the case of other investigated compounds, bearing the anthracene moiety, however, only trace signals were found.

The reaction in question appears to be hindered through substitution with the phenoxophen-2-yl moiety in *4f*, as we can observe as an EPR signal of the radical anion. Among the substituents to the anthracene group present in the investigated compounds, the phenoxophen-2-yl substituent most effectively shields the anthracene moiety sterically, indicating the reaction site. In this case characteristic line splitting is observed, due to the presence of a nitrogen atom in the system. The results of electrochemical study confirmed that anthracene moiety effectively interrupts communication between each group and leads to separated distributions of HOMO and LUMO levels, further illustrating that the bipolar design strategy employing an anthracene as the linkage can retain from violet to yellow emission and facilitate device operation as a result of a lower charge injection barrier. Therefore, the combination of anthracene-based, electron-transport materials gives the best performances in optical devices.

References

[1] Ai L., Ouyang X. H., Liu Q. D., Wang S. Y., Peng R. X., Islam A., Ge Z. Y., (2015). Effective side chain selection for enhanced open circuit voltage of polymer solar cells based on 2D-conjugated anthracene derivatives, Dyes and Pigments, 115: 73-80.

[2] Mallam V., Elbohy H., Qiao Q., Logue B. A., (2015). Investigation of novel anthracene-bridged carbazoles as sensitizers and Co-sensitizers for dye-sensitized solar cells, Int. J. Energy Res., 39: 1335–1344.

[3] Reid R. C., Minteer S. D., Gale B. K., (2015). Contact lens biofuel cell tested in a synthetic tear solution, Biosensors and Bioelectronics 68: 142–148.

[4] Prabhu J., Velmurugan K., Nandhakumar R., (2015). Development of fluorescent lead II sensor based on an anthracene derived chalcone, Spectrochimica Acta Part A: Molecular and Biomolecular Spectroscopy, 144: 23–28.

[5] Zhu Y. J. B., Duan J. C. X., (2015). Fluorescent Sensing of Fluoride in Cellular System, Theranostics, 5: 173-187.

[6] Srivastava P., Razi S. S., Ali R., Srivastav S., Patnaik S., Srikrishna S., Misra A., (2015). Highly sensitive cell imaging "Off–On" fluorescent probe for-mitochondria and ATP, Biosensors and Bioelectronics, 69: 179–185.

[7] Kim Y. S., Yoon J. Y., Lee H. W., Kim J., Lee H. W., Lee S. E., Kim Y. K., Yoon S. S., (2015). Blue fluorescent materials based on bis(10-phenylan-thracen-9-yl) derivatives containing heterocyclic moiety, Optical Materials, 46: 247–253.

[8] Song J. Y., Park S. N., Lee S. J., Kim Y. K., Yoon S. S., (2015). Novel fluorescent blue-emitting materials based on anthracene-fluorene hybrids with triphenylsilane group for organic light-emitting diodes, Dyes and Pigments, 114: 40–46.

[9] Zhang Z., Jiang W., Ban X., Yang M., Ye S., Huanga B., Sun Y., (2015). Solution-processed efficient deep-blue fluorescent organic light-emitting diodes based on novel 9,10-diphenyl-anthracene derivatives, RSC Adv. 5: 29708 -29717.

[10] Jang Y. J., Lim B. T., Yoon S. B., Choi H. J., Ha J. U., Chung D. S., Lee S.G., (2015). A small molecule composed of anthracene and thienothiophene devised for high-performance optoelectronic applications, Dyes and Pigments, 120: 30- 36.

[11] Liu J., Dong H., Wang Z., Ji D., Cheng C., Geng H., Zhang H., Zhen Y., Jiang L., Fu H., Bo Z., Chen W., Shuai Z., Hu W., (2015). Thin film field-effect transistors of 2,6-diphenyl anthracene (DPA), Chem. Commun., 51: 11777-11779.

[12] Yokokura S., Takahashi Y., Nonaka H., Hasegawa H., Harada J., Inabe T., Kumai R., Okamoto H., Matsushita M. M., Awaga K., (2015). Switching of Transfer Characteristics of an Organic Field-Effect Transistor by Phase Transitions: Sensitive Response to Molecular Dynamics and Charge Fluctuation, Chem. Mater. 27: 4441–4449.

[13] Pope M., Kallmann H. P., Magnante P., (1963). Electroluminescence in organic crystals J Chem Phys, 38: 2042–2043.

[14] Williams D. F., Schadt M., (1970). A Simple Organic Electroluminescent Diode, Proc. IEE, 58: 476

[15] Williams F., Schadt M., (1970). dc and Pulsed Electroluminescence in

Anthracene and Doped Anthracene Crystals Digby, J. Chem. Phys., 53: 3480-3487.

[16] Tang C. W., VanSlyke S. A., (1987). Organic electroluminescent diodes, Appl. Phys. Lett. 51: 913-915.

[17] Wu K. C., Ku P. J., Lin C. S., Shih H. T., Wu F. I., Huang M. J., Lin J. J., Chen I. C., Cheng C. H., (2008). The photophysical properties of dipyrenylbenzenes and their application as exceedingly efficient blue emitters for electroluminescent devices, Adv. Funct. Mater., 18: 67– 75.

[18] Huang J. H., Su J. H., Li X., Lam M. K., Fung K. M., Fan H. H., Cheah K. W., Chenb C. H. Tian H., (2011). Bipolar anthracene derivatives containing hole- and electron-transporting moieties for highly efficient blue electroluminescence devices, J Mater Chem, 21: 2957–2964.

[19] Zhuang S., Shangguan R., Huang H., Tu G., Wang L., Zhu X., (2014). Synthesis, characterization, physical properties, and blue electroluminescent device applications of phenanthroimidazole derivatives containing anthracene or pyrene moiety, Dyes and Pigments 101: 93–102.

[20] Zhang P., Dou W., Ju Z. H., Yang L. Z., Tang X. L., Liu W. S., Wu Y., (2013). A 9,9'-bianthracene-cored molecule enjoying twisted intramolecular charge transfer to enhance radiative-excitons generation for highly efficient deep-blue OLEDs, Org Electron 14: 915–925.

[21] Zając D., Sołoducho J., Jarosz T., Łapkowski M., Roszak S., (2015). Conjugated silane-based arylenes as luminescent materials, Electrochimica acta 173: 105-116.

[22] Łapkowski M., Golba S., Żak J., Stolarczyk A., Sołoducho J., Doskocz J., Sulkowski W. W., Bartoszek M., (2009). Polimery przewodzące zawierające jednostkę fenotiazynową w łańcuchu głównym, Polimery 54: 255.

[23] Vollmer F., Rettig W., Birckner E., (1994). Photochemical mechanisms producing large fluorescence stokes shifts, J. Fluoresc. 4: 65–69.

[24] Olech K., Sołoducho J., Laba K., Data P., Lapkowski M., Roszak S., (2014). The Synthesis and Characterization of -3,4-Ethylenedioxythiophene Derivatives with Electroactive Features, Electrochim. Acta 141: 349–356.

[25] Idzik K., Soloducho J., Cabaj J., Mosiadz M., Lapkowski M., Golba S., (2008). Development of structural characterization and physicochemical behaviour of triphenylamine blocks, Helv. Chim. Acta 91: 618- 627.

[26] University of Central Florida Research Foundation, Inc.; Phanstiel, IV, Otto (2013)Patent: US8410311 B1.

[27] Parr R. G., Yang W., (1994). Density Functional Theory of Atoms and Molecules, Oxford University Press, New York.

[28] Becke A.D., (1993). Density functional thermochemistry. III. The role of exact exchange, J. Chem. Phys. 98: 5648-5652.

[29] Vosco S. H., Wilk L., Nusair M., (1980). Accurate Spin-Dependent Electron Liquid Corre-lation Energies for Local Spin Density Calculations: A Critical Analysis, Can. J. Phys. 58: 1200-1211.

[30] Lee C., Yang W., Parr R.G., (1988). Development of the Colle-Salvetti correlation-energy formula into a functional of the electron density, Phys. Rev. B 37: 785.

[31] Dunning T.H., (1989). Gaussian basis sets for use in correlated molecular calculations. I. The atoms boron through neon and hydrogen, J. Chem. Phys. 90: 1007.

[32] Marques M. A. L., Ullrich C.A., Nogueira F., Rubio A., Burke K., Gross E.K.U. (Eds.) (2006). Time-Dependent Density Functional Theory, Springer-Verlag.

[33] Gaussian 09, Revision E.01, Frisch M. J., Trucks G. W., Schlegel H. B., Scuseria G. E., Robb M. A., Cheeseman J. R., Scalmani G., Barone V., Mennucci B., Petersson G. A., Nakatsuji H., Caricato M., Li X., Hratchian H. P., Izmaylov A. F., Bloino J., Zheng G., Sonnenberg J. L., Hada M., Ehara M., Toyota K., Fukuda R., Hasegawa J., Ishida M., Nakajima T., Honda Y., Kitao O., Nakai H., Vreven T., Montgomery J. A. Jr., Peralta J. E., Ogliaro F., Bearpark M., Heyd J. J., Brothers E., Kudin K. N., Staroverov V. N., Kobayashi R., Normand J., Raghavachari K., Rendell A., Burant J. C., Iyengar S. S., Tomasi J., Cossi M., Rega N., Millam J. M., Klene M., Knox J. E., Cross J. B., Bakken V., Adamo C., Jaramillo J., Gomperts R., Stratmann R. E., Yazyev O., Austin A. J., Cammi R., Pomelli C., Ochterski J. W., Martin R. L., Morokuma K., Zakrzewski V. G., Voth G. A., Salvador P., Dannenberg J. J., Dapprich S., Daniels A. D., Farkas Ö., Foresman J. B., Ortiz J. V., Cioslowski J., Fox D. J., (2009) Gaussian, Inc., Wallingford CT.

[34] GaussView 3.0, Gaussian, Inc., Carnegie Office Park – Building 6, Pittsburgh, PA, USA.